镁铝水滑石层板与层间阴离子相互作用的理论研究

罗青松 李 蕾 王作新 段 雪*
(北京化工大学可控化学反应科学与技术基础教育部重点实验室, 北京 100029)

本文采用以 ASED-MO(含原子对排斥的 EHMO 法) 为基础的结构自动优化的 EHTOPT 程序, 对镁铝水滑石(LDHs)层板与层间阴离子相互作用进行了理论研究。以 $Mg_6Al_2(OH)_{16}X \cdot H_2O$ 为分子结构单元, 计算并分析了与不同层间阴离子形成稳定结构的能量变化、成键状况及电荷转移情况, 揭示了层间作用力的本质。结果表明, LDHs 层板与层间阴离子间存在静电吸引、氢键等非共价键弱相互作用, 且氢键作用为主, 其强弱与阴离子电荷分布、空间排布方式密切相关; 层间阴离子电荷分布同时还影响着层板酸碱性的变化。

关键词: ASED-MO 方法 镁铝水滑石 水滑石 理论研究
分类号: O641.3

Theoretical Study of the Layer-Anion Interactions in Magnesium Aluminum Layered Double Hydroxides

LUO Qing-Song LI Lei WANG Zuo-Xin DUAN Xue*
(*Key Lab for Science and Technology of Controllable Chemical Reactions, Education Ministry, Beijing University of Chemical Technology, Beijing* 100029)

The interaction of the intercalated anions with the cationic sheets in magnesium aluminum layered double hydroxides has been investigated using the ASED-MO method. The energy changes, and the nature of the bonding have been studied during the formation of the layered structure with different anions, based on the model $Mg_6Al_2(OH)_{16}X \cdot H_2O$. The calculations have shown that both Coulombic and hydrogen bonding interactions exist in the layered structure, and the strength of the hydrogen bonding interaction is connected with the charge distribution of the anion and its orientation in space. Furthermore, it indicates that the variation in acid-base properties of the layers is affected by the charge distribution of the intercalated anion.

Keywords: **ASED-MO method** **Mg-Al hydrotalcites** **hydrotalcite** **theoretical study**

0 Introduction

Layered double hydroxides(LDHs, or the so-called anionic clays) consist of positively

收稿日期: 2001-05-28。收修改稿日期: 2001-07-09。
北京市自然科学基金资助项目(No. 2002016)。
*通讯联系人。
第一作者: 罗青松, 男, 26 岁, 硕士研究生; 研究方向: 层状结构材料。

charged brucite-like ($Mg(OH)_2$-type) layers separated by counter-anions and water molecules. The chemical composition of this class of intercalation compounds can be expressed in general as $[M^{Ⅱ}_{1-x}M^{Ⅲ}_x(OH)_2]^{x+}[A^{n-}]_{x/n} \cdot mH_2O$, where $M^{Ⅱ}$ and $M^{Ⅲ}$ are the divalent and trivalent cations in the octahedral interstices of the hydroxide layer and A^{n-} is the charge-balancing interlayer gallery anion. LDHs are an important class of materials currently receiving considerable attention[1] because of their large fields of application, for example as exchanger, catalysts or electrochemical sensors.

Many studies on the synthesis and properties of these materials have been carried out recently[2, 3], but there are few reports of investigation of the layer-anion interactions using quantum chemistry. In this work the layer-anion interactions are investigated using a semi-empirical method (EHMO), in order to understand these materials further.

1 Calculation Section

The theoretical study has been carried out using the EHTOPT package based on the ASED (Atom Superposition and Electron Delocalization)-MO method(EHMO including atomic repulsion energy)[4]. ASED-MO treats the energy E as a sum of E_D and E_R ($E = E_D + E_R$), where E_D is the electron energy calculated using the EHMO method and E_R is a sum of the repulsion energies E_{ab} of all atom-pairs in a molecule($E_R = \Sigma E_{ab}$). The EHMO parameters for the atoms used are listed in Table 1. All the structural parameters that are not optimized in the calculations come from the literature. The bond lengths are: C-O = 0.129nm[5], S-O = 0.149nm[5], Cr-O = 0.165nm[5], H-O = 0.0957nm[5], N-O = 0.124nm[6], Al-O = 0.190nm[7], Mg-O = 0.211nm[7].

Table 1 Parameters used in EHMO Calculation

atom	orbital	H_{ij}/eV	slater index
H	1*s*	-13.60	1.300
C	2*s*	-16.60	1.610
	2*p*	-11.30	1.570
N	2*s*	-20.30	1.920
	2*p*	-14.50	1.920
O	2*s*	-28.50	2.250
	2*p*	-13.60	2.230
Mg	3*s*	-7.60	1.103
	3*p*	-4.00	1.103
Al	3*s*	-10.60	1.372
	3*p*	-6.00	1.355
S	3*s*	-20.20	2.122
	3*p*	-10.40	1.827
Cr	3*d*	-8.30	4.950
	4*s*	-6.77	1.300
	4*p*	-3.70	1.300

The $Mg_6Al_2(OH)_{16}X \cdot H_2O$ unit is abbreviated as LDHs-X, where X refers to different intercalated anions. The structure of LDHs-X is optimized running on a 586 computer, and the energy changes, nature of bonding and charge transfer are studied during the formation of the layered structure with different anions, which gives some insight into the nature of the interactions between the layers and the intercalated anions.

2 Results and Discussion

2.1 Interaction between the Layers and the Intercalated Anion

2.1.1 Optimization of the Structure of LDHs-X

Our calculation model is based on experimental data[1,8] and is shown in Fig. 1, The numbers of the atoms of the cationic sheets in other figures are the same as in the basic structure for $Mg_6Al_2(OH)_{16}CO_3 \cdot H_2O$.

The energy changes have been calculated during the assembly of the layered structure with different anions. The relative energy change with the decrease in the gallery height for LDHs-CO_3 is shown in Table 2, and the overlap populations obtained from relevant atoms are given in Table 3.

Table 2　Energy Changes in the Process of Forming LDHs-CO_3

gallery height(d)/nm	E/eV	ΔE/eV
0.764	-2911.1082	0
0.564	-2911.4390	-0.3308
0.514	-2911.5173	-0.4091
0.464	-2911.5702	-0.4620
0.414	-2911.6239	-0.5157
0.364	-2911.6665	-0.5583
0.314	-2911.4332	-0.3250
0.264	-2910.8211	0.2871

Table 3　Overlap Populations for the Atoms Involved in the Assembly of LDHs-CO_3

gallery height(d)/nm	O_{41}-H_1	O_{41}-H_{21}	O_{43}-H_{17}	O_{43}-H_{37}	O_{44}-H_{15}	O_{44}-H_{35}
0.764	0.0000	0.0000	0.0000	0.0000	0.0000	0.0000
0.564	—	0.0233	—	0.0265	0.0030	—
0.514	—	0.0199	—	0.0228	0.0110	—
0.464	—	0.0160	—	0.0186	0.0225	—
0.414	0.0016	0.0155	0.0007	0.0204	0.0275	—
0.364	0.0140	0.0185	0.0154	0.0141	0.0151	0.0146
0.314	0.0462	0.0459	0.0087	0.0099	0.0072	0.0076
0.264	0.1269	0.1202	0.0083	0.0088	0.0067	0.0068

The total energy decreases gradually with decreasing gallery height without any obvious energy barrier, which indicates that the process is spontaneous. The planar carbonate anion changes from an orientation perpendicular to the plane of the sheets to one parallel to the plane of the sheets. The energy decrease is a result of increasing Coulombic interaction between the CO_3^{2-} ion and the ions of the layers, and increasingly strong hydrogen-bonding interactions between the oxygen atoms of the carbonate anion and the hydroxyl groups of the layers. Energy minimization gives a gallery height of 0.364nm. At shorter gallery heights, the energy increases as a result of the repulsion between the layer ions and intercalated anions at the shorter distances.

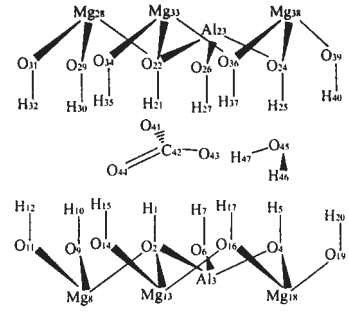

Fig. 1　Structure of $Mg_6Al_2(OH)_{16}X \cdot H_2O$

The relative energies and the gallery heights calculated for other anions, using the same model, are given in Table 4. The optimized gallery heights are basically in agreement with those obtained from experimental data[9].

Table 4 Energies and Gallery Heights of LDHs-X

compound	E_1/eV	E_2/eV	ΔE/eV	gallery height (d)/nm (Cal)	(Exp)
LDHs-NO_3	-3371.4278	-3371.7815	-0.3537	0.485	0.389[1]
LDHs-CO_3	-2911.1082	-2911.6665	-0.5583	0.364	0.293
LDHs-SO_4	-3052.0159	-3052.4252	-0.4093	0.480	0.384
LDHs-CrO_4	-3035.2453	-3037.6255	-2.3802	0.475	0.396

The overlap populations between the oxygen atom of intercalated water and the hydroxyl groups of the layer are given in Table 5. It can be seen that the interactions between them are weaker, and the water molecule is of less effect on the energy changes and the gallery height for the different LDHs. The effect may be more obvious when the number of the intercalated water molecule increases. It needs to be studied further in the future. We didn't discuss it in this paper owing to the limits of the model used.

Table 5 Overlap Populations between the Water Molecule and the Hydroxyl of the Layer of LDHs-X

LDHs-X	LDHs-NO_3		LDHs-CO_3		LDHs-SO_4		LDHs-CrO_4	
	O_{H_2O}-H_5	O_{H_2O}-H_{20}	O_{H_2O}-H_5	O_{H_2O}-H_{25}	O_{H_2O}-H_{25}	O_{H_2O}-H_{37}	O_{H_2O}-H_{17}	O_{H_2O}-H_{37}
	0.0064	0.0008	0.0094	0.0121	0.0275	0.0001	0.0150	0.0008

2.1.2 Analysis of the LDHs-X Structure

The calculated net charges on the constituent atoms of different isolated anions before the formation of the LDHs-X structure are shown in Table 6.

Table 6 Net Charges on the Atoms of Different Isolated Anions

anion	NO_3^-		CO_3^{2-}		SO_4^{2-}		CrO_4^{2-}	
	O_{NO_3}	N	O_{CO_3}	C	O_{SO_4}	S	O_{CrO_4}	Cr
	-0.8163	1.4489	-1.1503	1.4509	-1.2570	3.0279	-1.6413	4.5654

LDHs-CrO_4 The geometry of isolated CrO_4^{2-} anion is tetrahedral with T_d symmetry. The orientation of CrO_4^{2-} in the interlayer is shown in Fig. 2, and the overlap populations between the four oxygen atoms of the CrO_4^{2-} anion and the hydroxyl groups of the layer are given in Table 7. The calculations indicate that the oxygen atoms of the anion are hydrogen bonded to the hydroxyl groups of the layer. The higher the net charge on the oxygen atoms of the isolated anion, the stronger the hydrogen bonding interaction can be expected to be, and the greater the observed energy decrease expected. It can be seen that the net

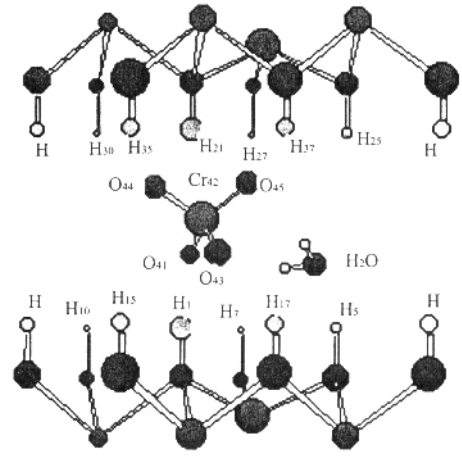

Fig. 2 Structure of $Mg_6Al_2(OH)_{16}CrO_4 \cdot H_2O$

charge on the anionic center in CrO_4^{2-} is higher than in any other anions(Table 6), and consequently, the hydrogen bonding interaction is much stronger, even though except for the NO_3^- all of the other anions are also divalent. It can be seen that the energy decreases accompanying the formation of the LDHs greatest in the case of CrO_4^{2-}(Table 4) . The fact that LDHs can be used to remove CrO_4^{2-} from waste-water[10] is consistent with that the formation of LDHs-CrO_4 is very energetically favorable.

Table 7　Overlap Populations for the Relevant Atoms of LDHs-CrO_4

O_{41}-H_1	O_{43}-H_{17}	O_{44}-H_{35}	O_{45}-H_{37}
0.0582	0.0461	0.0503	0.0432

LDHs-CO_3 Three hydroxyl groups around a c_3 axis perpendicular to the layers form an equilateral triangle, $\Delta 1$, with the length 0.303nm. Carbonate anion with symmetry D_{3h} is also an equilateral triangle, $\Delta 2$, with the length 0.234nm corresponding to the O-O distance. On energy minimization, $\Delta 2$ is found to be located in $\Delta 1$, with the c_3 axis of the anion is perpendicular to the sheets with the carbonate anion lying midway between the upper and lower sheets(Fig. 3). The distance of the three O_{anion} to the upper sheet is almost the same as that to the lower sheet, and the nature of the bonding to each sheet is similar(The overlap populations are shown in Table 3). Furthermore, the interactions between every O_{anion} and the hydroxyl groups of the layers have nearly the same strength. For example, O_{41}-H_1 = 0.0140 and O_{41}-H_{21} = 0.0185. In other words, the carbonate anion adopts a very symmetric orientation in the interlayer resulting in the observed large decrease in energy.

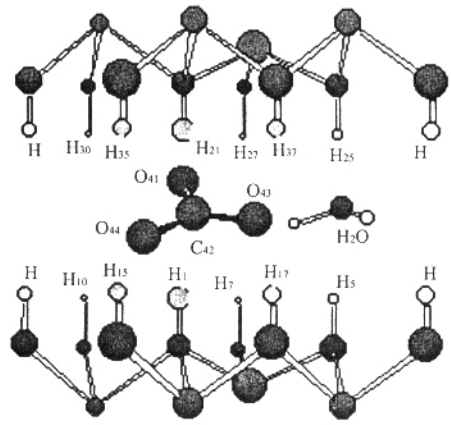

Fig. 3　Structure of $Mg_6Al_2(OH)_{16}CO_3 \cdot H_2O$

The orientation of CO_3^{2-} in the interlayer clearly gives the overall LDHs-CO_3 system a highly symmetric arrangement even though the net charge on the O_{anion} of carbonate anion is lower than in SO_4^{2-} or CrO_4^{2-}, which may be one reason why the most commonly observed LDHs is LDHs-CO_3.

LDHs-SO_4 The geometry of isolated sulfate anion is tetrahedral with T_d symmetry. In the interlayer, the sulfate anion may have two different orientations with respect to the planes of the hydroxyl ions, i. e. either the c_2 or c_3 axis lies perpendicular to the sheets, which is denoted as $C_2\perp$ or $C_3\perp$ respectively. The energy is −3052.4011eV for the former and −3052.4252eV for the latter, suggesting that the $C_3\perp$ structure is slightly more stable. The four oxygen atoms of the sulfate anion make a pyramidal orientation in the interlayer, in which three oxygen atoms of sulfate anion (O_{41}, O_{44}, O_{45},) are directed toward the lower layer, making a triangle(denoted $\Delta 3$), and the other one(O_{43}) points toward the opposite layer, making the top of the pyramid(Fig. 4). The overlap populations between the four oxygen atoms of sulfate anion and the hydroxyl groups of the layer are given in Table 8.

Table 8 Overlap Populations for the Relevant Atoms of LDHs-SO_4

O_{43}-H_{21}	O_{43}-H_{35}	O_{43}-H_{37}	O_{41}-H_1	O_{45}-H_{15}	O_{44}-H_{17}
0.0080	0.0057	0.0064	0.0386	0.0432	0.0471

As shown in Table 8, the interactions between the $\Delta 3$ and the hydroxyls of lower layer are very strong, and the nature of the bonding is similar in each case; the interaction between O_{43} and the hydroxyls of upper layer is weaker, however. It is clear that the nature of the bonding between the sulfate anion and the hydroxyl groups of opposite layers is very different. Compared with LDHs-CO_3, the configuration of LDHs-SO_4 will lead to a loss in symmetry, The energy decrease accompanying the formation of LDHs-SO_4 is much less than LDHs-CO_3, which is consistent with the observation that the sulfate anion is more readily exchanged by other ions[9].

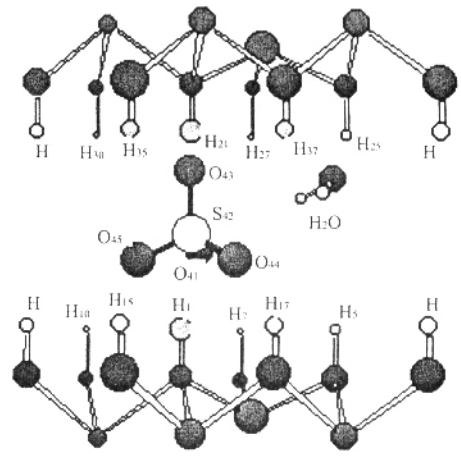

Fig. 4 Structure of $Mg_6Al_2(OH)_{16}SO_4 \cdot H_2O$

LDHs-NO_3 Although the geometry and size of NO_3^- is the same as CO_3^{2-}, the energy of LDHs-NO_3 is minimized when the c_3 axis of the ion adopts an orientation of approximately 60° to the layers(Fig. 5). The reason for this is that the nitrate anion is a monovalent ion so that the interlayer anion density is higher than in the case of LDHs-CO_3. There will be a strong steric repulsion, between the two nitrate anions, resulting in greater energy for the overall system, if NO_3^- is parallel to the sheets inside the crowded interlayer region. The NO_3^- ions have to tilt away from the sheets in order to minimize these repulsions.

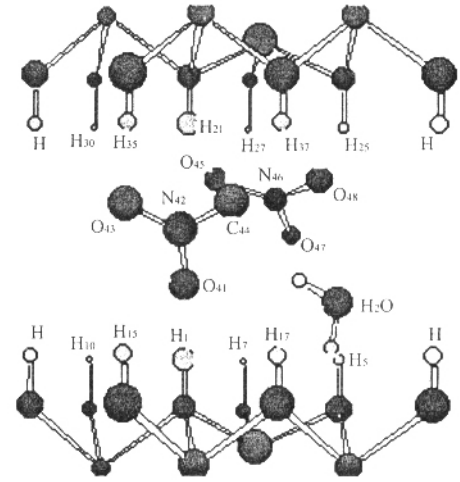

Fig. 5 Structure of $Mg_6Al_2(OH)_{16}(NO_3)_2 \cdot H_2O$

The gallery height(0.485nm) in the optimized LDHs-NO_3 structure is higher than that of LDHs-CO_3, owing to the nitrate anions adopting the skewed orientation. To take the nitrate anion with N_{41} as an example, the overlap populations between the Oanion and the OH of the sheets are H_1-O_{41} = 0.0036, H_{35}-O_{43} = 0.0280 and H_{37}-O_{44} = 0.0274. Compared with CO_3^{2-}, NO_3^- is closer to the upper layer, with a greatly decreased contact area between NO_3^- and the cationic sheets, and the interactions of NO_3^- with the opposite sheets are very different. We suggest that the lower symmetry will make the structure less stable which is consistent with the observation that the LDHs-NO_3 is the most easily substituted in a widely variety of LDHs[11].

2. 2　Influence of the Intercalated Anion Upon the Hydroxyls of the Layer

The calculations indicate that the intercalated anions, being far from the cations of the sheets, have a weak Coulombic attraction with the cations of the sheets. However, there is a strong predominantly hydrogen bonding interaction between the anions and the hydroxyls of the sheets. The net charge of both the hydroxyls of the sheets and the oxygen atoms of the intercalated anions changes after the layered structure is formed. To take H_1 of the hydroxyls and O_{anion} nearby as an example, their net charges are listed in Table 9.

Table 9　Net Charges for the Relevant Atoms of LDHs-X

compound	O_{anion}		H_1	
	isolated anion	(LDHs)	isolated layer	(LDHs)
LDHs-NO_3	- 0. 8163	- 0. 8050	0. 2371	0. 2325
LDHs-CO_3	- 1. 1503	- 1. 1133	—	0. 2341
LDHs-SO_4	- 1. 2570	- 1. 2188	—	0. 2336
LDHs-CrO_4	- 1. 6413	- 1. 5281	—	0. 2215

As shown in Table 9, both the negative charge of the O_{anion} atoms and the positive charge of the H atom of the hydroxyls are reduced, after the hydrogen bond between the anions and the cationic sheets is formed. This suggests that the O_{anion} atom is the electron-donor, while the H atom of the hydroxyls is the electron-acceptor, i. e. their relationship is $O_{anion} \rightarrow H$.

Both the bond lengths and the overlap populations of the hydroxyls of the sheets with different intercalated anions are listed in Table 10.

Table 10　Structural and Electronic Parameters of LDHs-X

compound	bond length/nm	overlap population	
	(H_{21}-O_{22})	(H_1-O_2)	(H_1-O_{anion})
LDHs-NO_3	0. 0927	0. 7971	0. 0036
LDHs-CO_3	0. 0930	0. 7915	0. 0140
LDHs-SO_4	0. 0937	0. 7728	0. 0386
LDHs-CrO_4	0. 0966	0. 7327	0. 1295

As shown in Table 10, the O_{anion}-H overlap population increases, while the O_{layer}-H overlap population decreases, when the net charge on the O_{anion} atoms increases. This indicates that the interactions between the intercalated anions and the cationic sheets are becoming stronger, whereas the intralayer O_{layer}-H bonding is becoming weaker.

All the bond lengths of the hydroxyls of the sheets are shorter than the normal length (0. 0957nm[5]), except for the LDHs-CrO_4. The O_{anion}-H overlap population is less than 0. 04, but that of O_{layer}-H is about 0. 8. Accordingly, the hydrogen bonding interaction between the intercalated anions and the OH of the layers is weaker than the intralayer O_{layer}-H interaction. The reduced O_{layer}-H bond length demonstrates some increase in basicity of the layers.

The O_{layer}-H bond length in LDHs-CrO_4 however is 0. 0966nm, which is longer than the length in the isolated layer and the O_{anion}-H, in addition, its overlap population is 0. 1295. This suggests that as a result of the higher charge of O_{anion}, the O_{layer}-H bonding is weakened which makes the H atoms of the hydroxyls be more readily donated, enhancing the acid property of the layer. This suggests that varying the intercalated anions can control the acid-base properties of the layer.

3 Conclusions

The following conclusions can be drawn from this study:

(1) Both Coulombic and hydrogen bonding interactions exist in the layered structure between the layers and the intercalated anions, and the strength of the hydrogen bonding interaction, being the predominant interaction, is connected with the charge distribution of the anion and its orientation in space.

(2) As the net charge of the O_{anion} atom of the intercalated anion increases, the bond length of the hydroxyls of the layers is increased, leading to enhanced acid-strength of the layers.

References

[1] Cavani F., Trifiro F., Vaccarri A. *Catal. Today*, **1991**, **11**, 173.

[2] DUAN Xue(**段 雪**), JIAO Qing-Ze(**矫庆泽**), LI Lei(**李 蕾**) *Chinese Patent*, *CN*99119385.7.

[3] LI Lei(**李 蕾**), ZHANG Chun-Ying(**张春英**), JIAO Qing-Ze(**矫庆泽**), DUAN Xue(**段 雪**) *Wuji Huaxue Xuebao*(*Chinese J. Inorg. Chem.*), **2001**, **17**(1), 113.

[4] LI Lei(**李 蕾**), WANG Zuo-Xin(**王作新**), WANG Xiao-Yun **王晓筠**), YUAN Guo-Qing(**袁国卿**) *Huaxue Xuebao*(*Acta Chimica Sinica*), **1998**, **56**(8), 747.

[5] ZHOU Gong-Du(**周公度**) *Structural Inorganic Chemistry*(**无机结构化学**), Beijing: Science Press, **1982**.

[6] WANG Zhi-Zhong(**王志中**), LI Xiang-Dong(**李向东**) *The Theory and Practice on the Semi-empirical Methods of Molecular Orbital*(**半经验分子轨道的理论和实践**), Beijing: Science Press, **1981**.

[7] Bellotto D., Elkaim E. *J. Phys. Chem.*, **1996**, **100**, 8527.

[8] Bookin A. S., Cherkashin V. I. *Clays and Clay Minerals.*, **1993**, **41**, 558.

[9] Sato T., Wakabayashi T., Shimada M. *Ind. Eng. Chem. Prod. Res. Dev.*, **1986**, **25**, 89.

[10] *U. S. Patent* 4752397.

[11] GUO Jun(**郭 军**), SUN Tie(**孙 铁**) *Gaodeng Xuexiao Huaxue Xuebao*(*Chem. J. Chinese Univ.*), **1995**, **16**(3), 346.